Multi-Microgrids Load Balancing through EV Charging Networks

Xi Chen, *Senior Member, IEEE*, Haihui Wang, Fan Wu, *Member, IEEE*, Yujie Wu, Marta C. González, Junshan Zhang, *Fellow, IEEE*

***Abstract*—Energy demand and supply vary from area to area where an unbalanced load may occur and endanger the system security constraints and cause significant differences in the locational marginal price (LMP) in the power system. With the increasing proportion of local renewable energy (RE) sources in microgrids that are connected to the power grid and the growing number of electric vehicle (EV) charging loads, the imbalance will be further magnified. In this paper, we first model the EV charging network as a cyber-physical system (CPS) that is coupled with both the transportation networks and the smart grids. Then we propose an EV charging station recommendation algorithm. With a proper charging scheduling algorithm deployed, the synergy between the transportation network and the smart grid can be created. The EV charging activity will no longer be a burden for power grids, but a load balancing tool that can transfer energy between the unbalanced distribution grids. The proposed system model is validated via simulations. The results show that the proposed algorithms can optimize the EV charging behaviors, reduce charging costs, and effectively balance the regional load profiles of the grids.**

***Index Terms*—Electric vehicle, smart grid, demand response, EV charging network, power distribution grid.**

I. Introduction

As the concept of a more extensive interconnection of the power system, or even a global energy internet, has been proposed and studied on a pilot basis to enhance the efficiency of the power system, while the microgrid technology, with its greater independence and resilience, is also being more widely deployed. In a multi-microgrid system, different energy attributes of each microgrid, e.g. the types of users (industrial, commercial, or residential), the proportion of RE penetration, the total capacity of the microgrid, etc., may lead to a significant difference in the load characteristic, spatially and temporally, and hence may cause the load imbalance in the multi-microgrid system [1], [2]. Based on the information in the electricity markets, operators of a traditional power grid maintain the equilibrium between the generation supply and the aggregate demand of all served regions [3]–[5]. In recent years, the penetration rates of renewable energy (RE) sources in the power grid are rapidly increasing. Due to the intermittent nature of RE sources, which are typical current sources, the increasing proportion of RE brings huge security risks to the operation of the power system [6], [7]. At the same time, the electric vehicle (EV) has become the trend of vehicle development. With the rapid development of EV charging technology, faster EV charging stations have been developing that has further promoted the popularization of EVs [8]. Most of the EV charging actives are done at home or at workplaces with alternating current (AC), but from a consumer's point of view, the development of public fast chargers, direct current (DC) charging stations, will have a significant impact on the use of EVs. Studies have shown that even with only 1-5 % of fast charging events, the usage of EV will be increased by 25 %. To a certain extent, the availability of these fast charging stations can help alleviate the "range anxiety" that is generally considered a consumer's hesitation to adapt EVs [9], [10]. Due to the uncertainty of EV charging behaviors, uncoordinated charging of a mass of EVs may lead to unforeseen effects on the operation of a power distribution network [11], [12]. Without proper coordination, the increasing proportion of local RE sources and the growing number of EV charging loads may further magnify the imbalance of a grid and pose higher system security risks. It is not necessary to have any correlation between the growth of RE and EV, but both the up-growths indeed not only endanger system security constraints but also may cause changes of the locational marginal price (LMP) and hence produce unnecessarily higher cost [13].

X. Chen is with GEIRI North America, 250 W. Tasman Dr. San Jose, CA, USA 95134. (Corresponding author: Xi Chen, xc@ieee.org)

H. Wang, and F. Wu is with School of Electronic Engineering, Beijing University of Posts and Telecommunications, Beijing, China 100876.

Y. Wu is with the Department of Mathematics and Statistics, Washington University in St. Louis, MO, USA 63130.

M. González is with Departments of City and Regional Planning and Civil and Environmental Engineering at the University of California, Berkeley, CA, USA 94720.

J. Zhang is with School of Electrical, Computer and Energy Engineering, Arizona State University, AZ, USA 85287.

This work is supported by SGCC Science & Technology Project: 5418-201958524A-0-0-00.

A. Literature Review and State-of-the-art

To address the above problems, efforts on the energy demand response (DR) and the EV charging planning have been made. In smart grids, the DR mechanism allows better exploitation of RE, and improves the resilience and flexibility of the grid with response to the LMP [14], [15]. EVs are acknowledged to be one of the primary focuses of DR programs. Demand-side energy consumption scheduling is proposed to reduce the peak-to-average ratio of the power system [16]. With the involvement of EVs in the DR, the electricity demand side management (DSM) has been proved to further benefit in improving the utilization of RE and the efficiency of the networks. Tushar [17] proposed a real-time DSM system to manage the RE and residential load of the microgrid based on predicted aggregate load. Wang [18] used the LMP in a tri-level scheduling model to guide the aggregated electricity consumption of air conditioners and EVs. Ren [19] demonstrated

This article has been accepted for publication in a future issue of this journal, but has not been fully edited. Content may change prior to final publication. Citation information: DOI 10.1109/JIOT.2021.3108698, IEEE Internet of Things Journal

the benefits of distribution networks from the DR under a real-time LMP through optimal scheduling of the EV aggregator. Most of the control schemes proposed in the DR treat the EV charging as an exogenous process, ignoring the mobility nature of EVs and the facts that the EV may be charged at different charging stations of the grid depending on economic preferences and travel constraints.

Meanwhile, there is a rich literature focuses on the problem of the network routing of EVs. Given the stochastic nature of EV arrivals at charging stations, one can optimize various objectives such as the revenue maximization or the waiting time minimization [4], [20], [21]. In [22], the EV charging activities with interactions with RE are modeled as independent Markov processes and the problem of optimal charging scheduling at charging stations is studied. In [23], a vehicle-to-grid (V2G) mobile energy network model is proposed to study the impact of the EV mobility on balancing smart grid demand. Alizadeh [24] studies the collective effects of large-scale integration of EVs on the power network and the transportation network to solve the path planning problem under static settings. Etesami [25] models the EV routing problem as a repeated game and proposed a distributed control framework to control and balance the electricity load in a distributed manner across the grid. In [26], the Internet-of-Things (IoT) is applied in the EV charging network management to improve the efficiency of the EV charging scheduling. The authors in [27] studies the impact of the network connectivity and motor location deployment on the robustness of the grid system under a complex grid structure, and showed that the robustness of the grid can be enhanced by modifying the network topology. Sun [28] formulates the charging scheduling problem of EVs in the transportation network as a graphic game, and studies the correlated equilibrium and Nash equilibrium of the joint strategy of EV participants to minimize the charging delay. The authors in [29] proposed an energy trading online double auction scheme among EVs in microgrids with location privacy protection.

The above works have laid a solid foundation for modeling, analyzing, and optimizing the EV charging systems from a network perspective. However, most of the studies focused on the overall characteristics of the power grid and EV charging loads, emphasizing the stability of the grid and minimizing charging cost, but ignoring the respective load contributions of the charging stations in the microgrid. Much of the works on the EV charging planning, the charging station selection, and the system optimization requires the involvement of the LMP as an evaluation factor and mainly focuses on global optimization. However, we know that in a regional grid, such as a multi-microgrid system, there may not always be timely tariff information available and it is not sufficient for the system to consider only the tariff influenced by the overall grid supply and demand, sometimes as the overall microgrid load is kept in balance but there may still be severe load imbalances within the system and cannot be guided simply by tariff information.

B. Contribution and Organization

The main contributions of the paper are listed below.

(1) An EV is a part of transportation networks, and a charging station is a part of power systems. Through the EV charging activities, the smart multi-microgrids and intelligent transportation networks are coupled. Imitating the structure of graphs, a cyber-physical model of the EV charging network is modeled with considerations of both the spatial and temporal distribution of the transportation network and the power grid, as well as the dynamics of the charging process of EV charging. Network analysis is carried out based on the proposed model.

(2) Aiming at the problem of the spatial and temporal imbalance of the power load within a multi-microgrid system, we propose a charging station recommendation algorithm with constraints of the power load degree of microgrids. The algorithm prevents a large-scale influx of EVs into a small number of charging stations for charging service and avoids the sharp increase of the charging load and hence optimizes scheduling to make all the load of microgrids in the area tends to be balanced and stabilized. By deploying the imbalance degree of the microgrid as a constraint, the EV charging location selection decision will not only consider the distance to the charging stations or use random assignment but will also regard EV charging process as a DR tool to balance the regional power load. Moreover, the proposed optimal algorithm can be implemented without the LMP information.

(3) A multi-microgrid system contains RE sources, consumption units, and hierarchical EV charging schemes with EV charging stations and EV charging aggregators is proposed. Smart EV charging scheduling can be achieved with the proposed system in the physical absence of the charging aggregator. The model is suitable for areas where local RE generation is abundant and the power supply with high reliability, self-healing, and robustness is required. Further, the proposed system can assist in the scheduling of the power load in the microgrid to achieve the load balance without the support of V2G.

The reminder of this paper is organized as follows. The notation used in the paper is given in Nomenclature. Section III introduces the system model of the EV charging networks. In Section IV, the dynamic power load balancing algorithm is presented. Simulation results are illustrated to show the effectiveness of the proposed system. We conclude the paper in Section VI.

II. Nomenclature

$\boldsymbol{V_E}$	Set of EVs.
$\boldsymbol{V_{C,j}}$	Set of EV charging stations connected to the jth charging aggregator.
$\boldsymbol{V_G}$	Set of EV charging aggregators.
$G(V,E)$	A graph G where V is the superset of the set of charging aggregators and EVs, and E is the set of links.
$\mathbf{R}$	Set of distance between EVs and charging aggregators.
N	Total number of nodes.
L	Total number links.
$N_{C,j}$	Total number of charging stations in a multiple microgrid system.

This article has been accepted for publication in a future issue of this journal, but has not been fully edited. Content may change prior to final publication. Citation information: DOI 10.1109/JIOT.2021.3108698, IEEE Internet of Things Journal

N_G	Total number of charging aggregators in a multiple microgrid system.
N_E	Total number of EVs.
$V_{E,i}$	The ith EV.
$V_{G,j}$	The jth EV charging aggregator.
$\mathbf{V}_G^i$	Charging aggregator candidates that meet the driving range requirements, for EV $V_{E,i}$.
$B_{ini,i}$	Initial EV battery SoC for $V_{E,i}$ (%).
$B_{arr,i}$	EV battery SoC for $V_{E,i}$ when arrives at charging station (%).
R_{ij}	Distance between $V_{E,i}$ and $V_{G,j}$
R_{max}	Maximum driving distance of EVs.
C_j	Service capacity of a microgrid j.
$P_j(t)$	Real-time power of a microgrid j at time t.
$D_j(t)$	Load demand degree of a microgrid j at time t.
v	Average driving speed of EVs.
p	Charging power of fast charging stations.
E_r	Energy consumption spends on the way to charging stations.
Φ	Total charging time for fully charging EVs.
ΔT_{ij}	Traveling time duration for EV $V_{E,i}$ to a charging station belongs to the charging aggregator $V_{G,j}$.
$T_{ini}^{i,j}$	Charging time duration of EV $V_{E,i}$ which is served by $V_{G,j}$ for its SoC from 0 to $B_{arr,i}$.
a, b, c	Scale coefficients of charging process in the battery charging function.
η	Valley-to-peak ratio of a multi-microgrid system.
P_{valley}	Minimum load of a multiple microgrid system.
P_{peak}	Maximum load of a multiple microgrid system.
μ, σ, ν	Time parameter, scale parameter, and shape parameter in a probability density function of Φ.
φ	Upper threshold of the load demand.

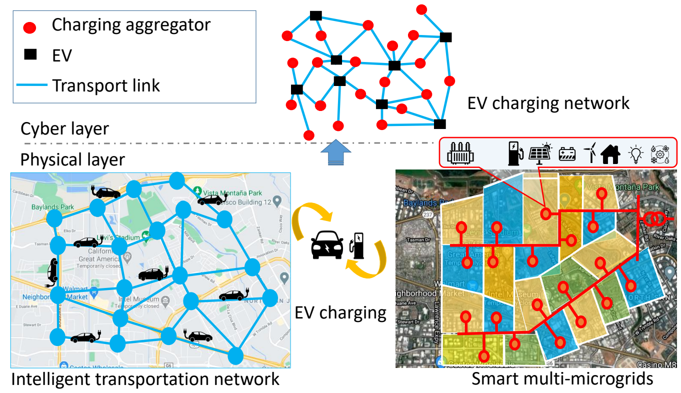

Fig. 1. An illustration of the cyber-physical EV charging network model. In the subfigure of the smart microgrids, each block represents a microgrid, and the red circle represents a substation. Connected by the red power lines, the electrical equipment in the microgrid, including charging stations, and the power generation units will be connected to the substation through which the grid is connected to. In the subfigure of the intelligent transportation networks, the blue circle represents a road traffic intersection, and the blue line represents the road traffic link. In the graph model, EVs and charging stations form the nodes, and the links are the road transportation between EVs and charging stations. In the graph model, the charging station node is not a single charging station port or station but a set that includes all the charging station charging ports under the power substation.

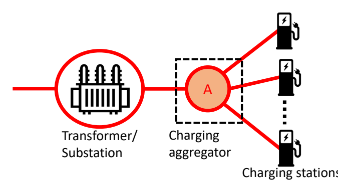

Fig. 2. An illustration of the charging aggregator in a microgrid. All charging stations within the same microgrid are connected to a charging aggregator which can be either a power flow aggregator or a virtual one which is functionally played by the transformer of the substation in the microgrid.

III. System Model

A. EV Charging Network

Given an EV charging network, EVs and charging aggregators (charging stations) are regarded nodes, and the roads between them are regarded as edges. Therefore, the topology of the EV charging network can be expressed as a directed graph $G(V, E)$ where V is a set of nodes and E is the set of links. Moreover, V is the superset of the set of charging aggregators, V_G, and the set of EVs, V_E, i.e. $V = V_G \cup V_E$. The total number of nodes and links is N and L, respectively. Specifically, we denote the number of charging aggregators and EVs as N_G and N_E, respectively. $N = N_G + N_E$, $L = N_G \times N_E$. N indicates the network size. Fig. 1 illustrates the model of an EV charging network through which the traffic flows in the intelligent transportation networks and the power flows in the smart microgrids are coupled. A microgrid in the model consists of the power load units, RE resources, and the EV charging infrastructures.

For simplicity, we assume all EV charging stations within a microgrid are connected to an EV charging aggregator which is located at the same node with the substation or transformer of that microgrid. As shown in Fig. 2, a charging aggregator is modeled as the summation of all EV charging stations in the microgrid. We assume that there is one and only one charging aggregator in each microgrid. The charging aggregator we deployed in this paper can be either a simple power flow aggregator or a virtual one that is functionally played by the transformer of the substation in the microgrid. The total number of EV charging stations is $N_C = \sum_{j=1}^{N_G}(N_{C,j})$. If all charging stations are considered as nodes in the networks then the number of nodes N will increase exponentially. Hence, in the graph network computational model, we only consider the nodes of the charging aggregators and EVs.

Considering the geographical locations of the nodes V_G and V_E in the spatial analysis of the network, the distance between them represents the required travel distance for an EV to the charging stations. An $N_E \times N_G$ matrix $\mathbf{R}$, defined in (1), is used to describe the connectivity and the distance between

This article has been accepted for publication in a future issue of this journal, but has not been fully edited. Content may change prior to final publication. Citation information: DOI 10.1109/JIOT.2021.3108698, IEEE Internet of Things Journal

nodes, defined as follows,

$$\mathbf{R} = \begin{pmatrix} R_{11} & R_{12} & \dots & R_{1N_G} \\ R_{21} & R_{22} & \dots & R_{2N_G} \\ \vdots & \vdots & \ddots & \vdots \\ R_{N_E 1} & R_{N_E 2} & \dots & R_{N_E N_G} \end{pmatrix}, \quad (1)$$

in which R_{ij} is the distance between the nodes $V_{E,i}$ and $V_{G,j}$.

The distance between EVs and charging stations, $\mathbf{R}$, plays a key role in selecting a charging station for an EV driver. When the state of charge (SoC) of an EV is low, the driver will consider charging the EV. In this paper, we consider the cases that EVs are only charged at public fast DC charging stations. Normally, a closer charging station gains a higher possibility of being deployed by an EV driver. Our objective is to balance the load demand within all local microgrids, hence, other than the distance to the charging stations, the power load of local microgrids will be taken into considerations in EV charging dispatching. It should be noted that the model does not require the charging stations to be geographically adjacent, in fact, they can be in any location as long as they are electrically connected.

Furthermore, there are some assumptions we made in this paper. First, we assume that the charging stations powered by the same substation and the RE sources connected to the same substation all belong to the same microgrid and they are spatial identical. Second, we assume EVs will follow the dispatching recommendation from the system. As it is possible to incentive EV drivers to follow the dispatch suggestions [30], it is safe to say that the assumption is fair, reasonable, and feasible. Third, we assume there will be sufficient enough charging ports at a charging station, hence, no queue and zero waiting time for charging services.

B. Battery SoC Dynamics

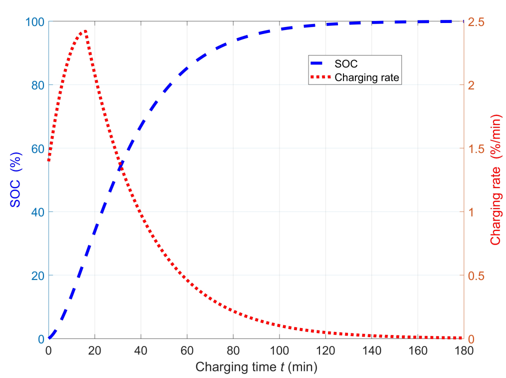

Fig. 3. Charging curve for DC charging method. The parameters setting is from [31]

The charging power of the fast charging station is generally 30 kW and above. Depending on the battery size, it takes about $2 \sim 3$ hours to fully charge an EV. The fast charging process is highly nonlinear. To capture the dynamics of the SoC in a charging process, we adopt a biexponential model in [31]:

$$SOC(t) = 1.0 + ae^{-bt} - (1+a)e^{-ct}, \quad (2)$$

where $SOC(t)$ is a nonlinear function gives the SoC of the EV at time t, and a, b and c are scale coefficients of the charging process. Both the battery charging and discharging processes are nonlinear. The charging process affects the grid as a power load, whose curve directly determines the charging time. The discharging process has minor direct impacts on the grid. In this paper, we focus on the charging process.

C. Load Demand Function

A local microgrid is interconnected to higher levels voltage power grids through a substation by which the charging stations are served and the RE sources are connected. Each microgrid has a maximum service capacity limited by its equipment, such as the transformers or the transmission lines. With the help of the dynamic capacity-increase technology and the incorporation of the RE power supply, the service capacity of the microgrid can be dynamically increased under certain conditions, however, generally speaking, the service capacity is predetermined at the stage of grid design and planning. In the actual operation of the grid, speaking of the operation cost and safety, the absolute value of real-time power is essential, but what is equivalently important is the relative demand degree of the capacity. A demand degree provides operating states information of the grid. When a demand degree is too high, a grid might reach its security thresholds. On the contrary, a low demand degree implies inefficient and uneconomic operation.

We denote the real-time demand degree of a microgrid as:

$$D_j(t) = P_j(t)/C_j, j \in \mathbf{V_G}, \quad (3)$$

where $D_j(t)$, C_j and $P_j(t)$ are the relative demand degree, the service capacity, and the real-time power consumption of a microgrid, respectively. Note that the demand degree does not reflect the absolute value of demand, but rather the relative demand in the microgrid. The relative demand is more important to a microgrid operator than the absolute demand because the security boundary is also the electricity usage associated with the capacity of that microgrid.

D. EV Charging Dynamics

When an EV driver decides to find a charging station for charging. There are two factors that bound the possible charging stations. One is the distance between the EV $V_{E,i}$, and the charging station $V_{G,j}$, and the other is the EV's SoC. The constraint condition for selecting charging stations is as follows.

$$R_{ij} \le R_{max} B_{ini,i}, \quad (4)$$

where R_{max} is the maximum driving range of the EV with a fully charged battery, and $B_{ini,i}$ is the current SoC of EV $V_{E,i}$. $R_{max} B_{ini,i}$ gives the furthest distance an EV can drive with its SoC. The battery consumption process is in fact also nonlinear and can sometimes be characterized by sudden drops in the SoC. We do not consider the dynamics of battery consumption.

This article has been accepted for publication in a future issue of this journal, but has not been fully edited. Content may change prior to final publication. Citation information: DOI 10.1109/JIOT.2021.3108698, IEEE Internet of Things Journal

Only the upper limit is constrained. Thus, the inequality (4) holds. The set of charging station candidates ($\mathbf{V}_G^i$) for $V_{E,i}$ is:

$$\mathbf{V}_G^i = \{V_{G,j} | R_{ij} \leq R_{max} B_{ini,i}\}, \tag{5}$$

An EV $V_{E,i}$ selects its charging station $V_{G,j}$ for charging. $B_{arr,i}$, the SoC of the EV reaching the charging station is given by:

$$B_{arr,i} = B_{ini,i} - E_{r,i} \tag{6}$$

where $E_{r,i}$ is the energy consumed by driving on the way to the charging station. If the consumption of the SoC is linear, then,

$$E_{r,i} = \frac{R_{ij}}{R_{max}}. \tag{7}$$

The traveling time to the charging station, ΔT_{ij}, is given by:

$$\Delta T_{ij} = \frac{R_{ij}}{v}, \tag{8}$$

where v is the average driving speed of the EV.

When an EV arrives at charging station for charging, its remaining SoC is $B_{arr,i}$. It will take the charging time of $T_{ini}^{i,j}$ for the SoC of the EV to charge from 0 to $B_{arr,i}$. The relationship between $B_{arr,i}$ and $T_{ini}^{i,j}$ is shown in (9).

$$B_{arr,i} = SOC(T_{ini}^{i,j}). \tag{9}$$

The time duration to fully charge an EV is denoted as Φ. Φ is not a constant, but a function that approximately conforms to the time-scale distribution. Follows [32], Φ is modeled as follows.

$$f_\Phi(t|\mu,\sigma,\nu) = \frac{\Gamma(\frac{\nu+1}{2})}{\sigma\sqrt{\nu\pi}\Gamma(\frac{\nu}{2})} \left[\frac{\nu + ((t-\mu)/\sigma)^2}{\nu}\right]^{-\frac{\nu+1}{2}}, \tag{10}$$

in which $f(\cdot)$ represents the probability density function of Φ, $\Gamma(\cdot)$ is the chi-square distribution, and μ, σ and ν are the time parameter, the scale parameter, and the shape parameter, respectively.

Given an EV at the time moment t_i, it will reach the charging station $V_{G,j}$ at the time moment t_j, thus,

$$t_j = t_i + \Delta T_{ij}. \tag{11}$$

When selecting a charging station, if (4) is satisfied, in the set $\mathbf{V}_G^i$, the EV $V_{E,i}$ will further consider $D(t)$ as another constraint.

$$D_j(t) \leq \varphi \qquad t \in (t_j, t_j + \Phi - T_{ini}^{i,j}), \tag{12}$$

where $D_j(t)$ is the load demand degree of the j microgrid at time t and φ is the upper threshold of the load demand.

For $V_{G,j} \in V_G^i$, the power of the charging stations $P_j(t)$ is as:

$$P_j(t) = \begin{cases} P_j(t) + p, & t \in (T_j, T_j + \Phi - T_{ini}^{i,j}), \\ P_j(t), & others, \end{cases} \tag{13}$$

where p is the charging power of the charging station.

IV. Load Balancing Algorithm

Our main goal is to balance the load between the areas in the distribution grids and to reduce the load difference of the microgrids. The valley-to-peak ratio (VTPR) of a multi-microgrid system is defined as $\eta(t)$ and given in (14).

$$\eta(t) = P_{valley}(t)/P_{peak}(t) \times 100\%, \tag{14}$$

in which $P_{valley}(t)$ and $P_{peak}(t)$ are the minimum and maximum load of a multi-microgrid system at time t, respectively. VTPR reflects the load difference degree among all the microgrids in the multi-microgrid system. A larger VTPR indicates the multi-microgrid is in a relatively balanced state, and there is no extreme difference between the load valleys and peaks. That is beneficial to the economic and safe operation of the microgrids.

The matching of EVs and charging stations is a game problem. By Properly assigning charging stations to EVs, the VTPR of the multi-microgrid can be enhanced. The load balancing matching strategy (LBMS) algorithm is described in Algorithm 1. First, it calculates the distance of the EV to all charging stations, and gets the set of available charging stations; then it selects a charging station with the lowest load demand degree among all available charging stations.

Algorithm 1: Load Balancing Matching

Input: EV information: location, time, SoC and speed; charging station information: location, power and microgrid load status;
Output: Matched charging station;
Calculate the distance matrix $\mathbf{R}$, $D_j(t)$;
for $V_{E,i} \in V_E$ **do**
  for $V_{G,j} \in V_G$ **do**
    if $R_{ij} \leq R_{max} B_{ini,i}$ **then**
      $V_{G,j} \in \mathbf{V}_G^i$;
    end
  end
  Choose the charging station $V_{G,j}$ from $\mathbf{V}_G^i$ with the lower power $P_j(t)$;
  for $t \in (t_j, t_j + \Phi - T_{ini}^{i,j})$ **do**
    if $D_j(t) \geq \varphi$ **then**
      delete $V_{G,j}$ from $\mathbf{V}_G^i$;
      Choose the charging station $V_{G,j}$ from $\mathbf{V}_G^i$ with the lower power $P_j(t)$ again;
    end
  end
  $P_j(t) = P_j(t) + p$;
end

V. Simulation Results

We set up simulations in MATLAB to verify the proposed algorithm and compared with the other two charging station assigning schemes, which are the random matching strategy (MRS) and the shortest distance matching strategy (SDMS). Follows [30]–[33], the parameters settings in the simulations

This article has been accepted for publication in a future issue of this journal, but has not been fully edited. Content may change prior to final publication. Citation information: DOI 10.1109/JIOT.2021.3108698, IEEE Internet of Things Journal

are given in TABLE I. The charging stations/aggregators are set to be evenly distributed in the area of 10 km $\times$ 10 km.

The actual data of electricity demand in California, USA are deployed as the basis of load information in simulation verification [34]. After being scaling down, the electricity demand data are randomly assigned to the 100 microgrids.

TABLE I
SIMULATION PARAMETER SETUP

Parameter	Value	Parameter	Value
a	2.096	b	0.0669
c	0.0469	μ	156.81
σ	5.40	ν	2.16
φ	0.9	v	30 km/h
p	50 kW	N_G	100
R_{max}	300 km	N_C	100

Combined with the given simulation parameters, the distribution of the full charge time Φ is shown in Fig. 4.

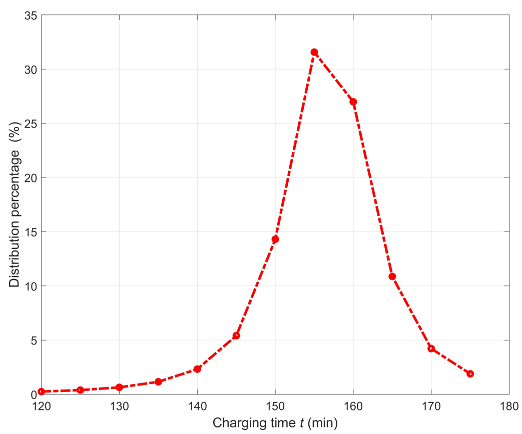

Fig. 4. Distribution percentage vs. Charging time t

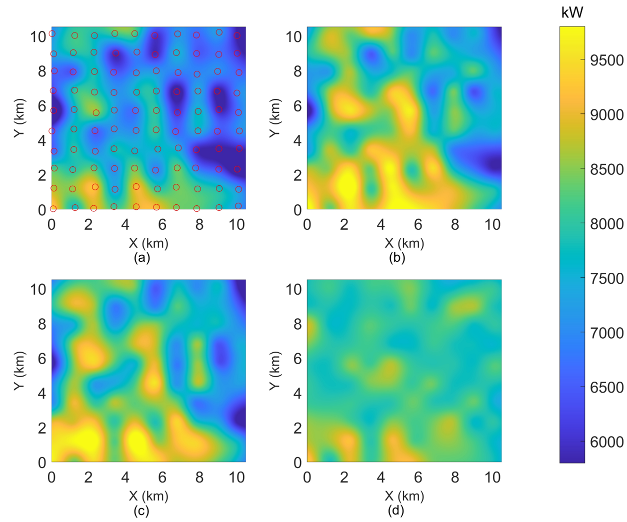

Fig. 5. Heat maps of the power load at 20:00 under different charging station recommendation strategies: (a) initial load (no EV charging), (b) the RMS, (c) the SDMS, and (d) the proposed LBMS.

Fig. 5 shows the power load of the multi-microgrid system at 20:00 under different charging station recommendation schemes with 16,000 EVs and 100 charging stations. The red circles in Fig. 5(a) represent the locations of charging stations. As shown in Fig. 5(a), the initial power distribution of the multi-microgrid system is extremely imbalanced, and there are peaks and valleys at different charging station locations. From Fig. 5(b) and (c), it can be seen the RMS and the SDMS cannot effectively fill the demand valley with EV charging loads. Oppositely, in some areas, the power peaks are strengthened.

That is the opposite of our optimization target. From Fig. 5(d), it can be clearly seen that the locations of the initial power valley (deep blue) have favorably been filled, and most of the load is within the range of $7,500 \sim 9,000$ kW. This shows that the proposed LBMS guides EVs to choose the charging stations in lower power demand microgrids, and hence effectively balances the load among the 100 microgrids.

Fig. 6 shows the accumulated daily energy consumption distribution of 16,000 EVs and 100 charging aggregators. Through Fig. 6(b) and Fig. 6(c), the RMS and the SDMS have failed to fill the energy valleys. Contrarily, in some locations, the load of the energy peak increased. The minimum energy density is about 1.3×10^5 kWh, the largest value is almost 2.0×10^5 kWh. Shown in Fig. 6(d), the initial energy valleys of the charging station have been well filled, and the energy density ranges in $1.6\times \sim 1.9 \times 10^5$ kWh. The results indicate that the proposed LBMS has led the EVs to charge at the places where the energy density is low. The EV charging load not only does not reinforce the peaks microgrid load in a multi-microgrid system but also fills the microgrid trough. Therefore, from the perspective of the multi-microgrid system, under LBMS, the energy consumption of charging stations promotes the load distribution of the multi-microgrid system towards balance.

In this study, there is no requirement for the power system to be V2G enabled. Knowing that V2G is still not enabled in most utilities. It is not due to technical problems of not considering V2G, but regulatory reasons. The proposed system will not have the ability to reduce load peaks, but can only improve the utilization in the low demand areas, if V2G is disabled in the system. Yet, simulation has illustrated great capability in load balancing of the proposed system in V2G disabled systems.

Under the RMS, an EV selects charging stations randomly. Under the SDMS, the nearest charging station from charging stations sets will be selected. Fig. 7 shows the comparisons results of η of different matching strategies with a different numbers of EVs, N_E of a 100 charging aggregators multi-microgrid system. while N_E increases, η under the RMS and the SDMS are both gradually decreasing, which reflects that the gaps between the peak and valley load of microgrids are widening and that may have negative impact on the safety and stable operation of the power grid. Contrariwise, the LBMS makes η gradually rise, while the number of EVs increases, indicating that the load gaps between the peak and the valley are narrowing, and the load demand among the microgrids in the multi-microgrid system is balanced.

This article has been accepted for publication in a future issue of this journal, but has not been fully edited. Content may change prior to final publication. Citation information: DOI 10.1109/JIOT.2021.3108698, IEEE Internet of Things Journal

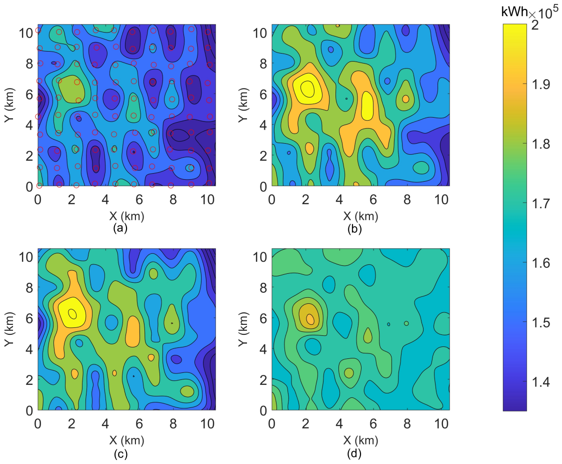

Fig. 6. Contour plots of accumulated daily energy consumption distribution under different charging station recommendation strategies: (a) initial load (no EV charging load), (b) the RMS, (c) the SDMS, and (d) the proposed LBMS.

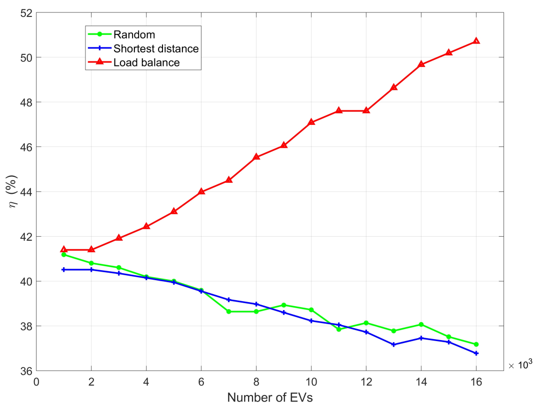

Fig. 7. Comparisons of η with the numbers of EVs.

The load standard deviation shows the severity of the fluctuation of the charging stations load. Smaller deviation means that the real-time load fluctuation of the charging stations is weak and the load is relatively stable, which is beneficial to the safe operation of the microgrid. Shown in Fig. 8, as the number of EVs increases, the load standard deviation under the RMS and the SDMS will rise, which indicates the fluctuation of the load is becoming severer. Instead, the load standard deviation drops significantly under the LBMS, which shows that proposed algorithm can better balance the load fluctuations of the charging stations.

Fig. 9 compares η of different charging stations recommendation strategies at different periods of the day. Compared to the RMS and the SDMS, η has been greatly improved under the LBMS. Even in the period when the η of the above two strategies is low, it can still increase η significantly, which shows that it can effectively balance the grid load and enhance the safety and stability of the grid operation at all time.

When prioritizing the charging station recommendations, because the RMS, the SDMS, and the LBMS have considered the distance between EVs and charging stations with different weights, the ultimate distance between the EV and the charging station will also be different. Fig. 10 shows the histogram of the driving distance to the charging stations under the three strategies with 16,000 EVs and 100 charging stations. As it can be seen from Fig. 10, under the SDMS, EVs select the nearest charging stations, and the driving distance are all within 10 km. The driving distance to the recommended charging stations under the RMS and the LBMS is statistically similar.

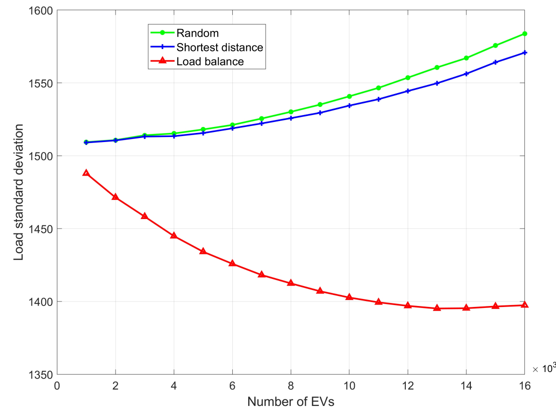

Fig. 8. Comparison of load standard deviation with the number of EVs.

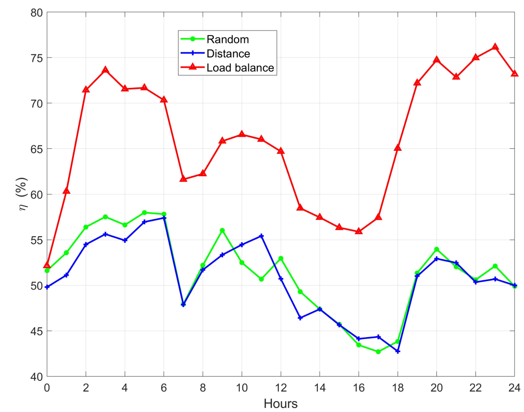

Fig. 9. Comparisons of η in a day.

VI. Conclusion

In this paper, based on graph theory, we modeled EV charging networks by coupling smart grids with intelligent transportation networks. A load balancing algorithm for multi-microgrid systems through EV charging station selection was proposed. By analyzing the distance factors between EVs and charging stations, and the statues of the microgrid load demands, the proposed algorithm can match an EV with a suitable charging station for charging. Simulation results showed that compared with the random matching and the shortest distance matching, the proposed load balancing algorithm can effectively reduce the peak-valley difference in multi-

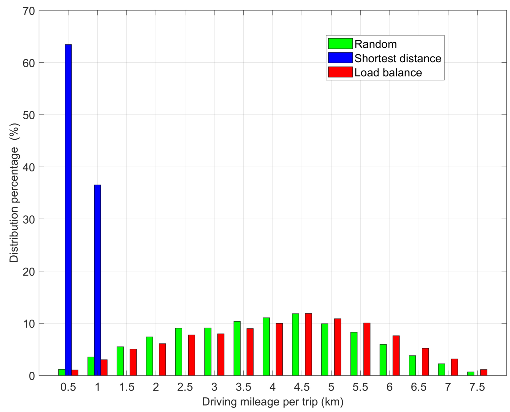

Fig. 10. Driving mileage per charging trip.

microgrid systems, and reasonably distribute EVs to charging stations. The proposed system can work effectively without V2G support.

REFERENCES

[1] Y. Du, Z. Wang, G. Liu, X. Chen, H. Yuan, Y. Wei, and F. Li, "A cooperative game approach for coordinating multi-microgrid operation within distribution systems," *Applied Energy*, vol. 222, pp. 383 – 395, Jul. 2018.

[2] B. Zhao, X. Wang, D. Lin, M. M. Calvin, J. C. Morgan, R. Qin, and C. Wang, "Energy management of multiple microgrids based on a system of systems architecture," *IEEE Trans. Power Syst.*, vol. 33, no. 6, pp. 6410–6421, Nov. 2018.

[3] F. Zhou, Y. Chen, and S. H. Low, "Sufficient conditions for exact semi-definite relaxation of optimal power flow in unbalanced multiphase radial networks," in *Proc. 2019 IEEE 58th Conf. Decision Cont.*, Dec. 2019, pp. 6227–6233.

[4] Q. Peng and S. H. Low, "Distributed optimal power flow algorithm for radial networks, I: Balanced single phase case," *IEEE Trans. Smart Grid*, vol. 9, no. 1, pp. 111–121, Jan. 2018.

[5] C. Yang, J. Yao, W. Lou, and S. Xie, "On demand response management performance optimization for microgrids under imperfect communication constraints," *IEEE Internet Things J.*, vol. 4, no. 4, pp. 881–893, Aug. 2017.

[6] C. K. Tse, M. Huang, X. Zhang, D. Liu, and X. L. Li, "Circuits and systems issues in power electronics penetrated power grid," *IEEE Open J. Circuits Syst.*, vol. 1, pp. 140–156, Sep. 2020.

[7] E. Barbour, D. Parra, Z. Awwad, and M. C. González, "Community energy storage: A smart choice for the smart grid?" *Applied Energy*, vol. 212, pp. 489 – 497, Feb. 2018.

[8] X. Chen, Z. Li, H. Dong, Z. Hu, and C. Chris Mi, "Enabling extreme fast charging technology for electric vehicles," *IEEE Trans. Intell. Transp. Syst.*, vol. 22, no. 1, pp. 466–470, Jan. 2021.

[9] H. Tu, H. Feng, S. Srdic, and S. Lukic, "Extreme fast charging of electric vehicles: A technology overview," *IEEE Trans. Transp. Electrific.*, vol. 5, no. 4, pp. 861–878, Dec. 2019.

[10] D. Howell, S. Boyd, B. Cunningham, S. Gillard, and L. Slezak, "Enabling fast charging: A technology gap assessment," U.S. Department of Energy, Tech. Rep., Oct. 2017. [Online]. Available: https://www.energy.gov/eere/vehicles/downloads/enabling-extreme-fast-charging-technology-gap-assessment

[11] Y. Xu, S. Çolak, E. C. Kara, S. J. Moura, and M. C. González, "Planning for electric vehicle needs by coupling charging profiles with urban mobility," *Nature Energy*, vol. 3, pp. 484–493, Apr. 2018.

[12] Y. Cao, T. Wang, O. Kaiwartya, G. Min, N. Ahmad, and A. H. Abdullah, "An EV charging management system concerning drivers' trip duration and mobility uncertainty," *IEEE Trans. Syst., Man, Cybern., Syst.*, vol. 48, no. 4, pp. 596–607, Apr. 2018.

[13] K. Zheng, Q. Chen, Y. Wang, C. Kang, and L. Xie, "Unsupervised congestion status identification using lmp data," *IEEE Trans. Smart Grid*, vol. 12, no. 1, pp. 726–736, Jan. 2021.

[14] S. C. Chan, K. M. Tsui, H. C. Wu, Y. Hou, Y. Wu, and F. F. Wu, "Load/price forecasting and managing demand response for smart grids: Methodologies and challenges," *IEEE Signal Process. Mag.*, vol. 29, no. 5, pp. 68–85, Sep. 2012.

[15] C. Cecati, C. Citro, and P. Siano, "Combined operations of renewable energy systems and responsive demand in a smart grid," *IEEE Trans. Sustain. Energy*, vol. 2, no. 4, pp. 468–476, Oct. 2011.

[16] Y. Liu, C. Yuen, S. Huang, N. Ul Hassan, X. Wang, and S. Xie, "Peak-to-average ratio constrained demand-side management with consumer's preference in residential smart grid," *IEEE J. Sel. Topics Signal Process.*, vol. 8, no. 6, pp. 1084–1097, Dec. 2014.

[17] M. H. K. Tushar, A. W. Zeineddine, and C. Assi, "Demand-side management by regulating charging and discharging of the EV, ESS, and utilizing renewable energy," *IEEE Trans. Ind. Informat.*, vol. 14, no. 1, pp. 117–126, Jan. 2018.

[18] X. Wang, F. Li, J. Dong, M. M. Olama, Q. Zhang, Q. Shi, B. Park, and T. Kuruganti, "Tri-level scheduling model considering residential demand flexibility of aggregated HVACs and EVs under distribution LMP," *IEEE Trans. Smart Grid*, pp. 1–1, 2021, doi=10.1109/TSG.2021.3075386.

[19] H. Ren, A. Zhang, F. Wang, X. Yan, Y. Li, N. Duić, M. Shafie-khah, and J. P. Catalão, "Optimal scheduling of an ev aggregator for demand response considering triple level benefits of three-parties," *Int. J. Elec. Power & Energy Syst.*, vol. 125, p. 106447, Feb. 2021.

[20] P. Fan, B. Sainbayar, and S. Ren, "Operation analysis of fast charging stations with energy demand control of electric vehicles," *IEEE Trans. Smart Grid*, vol. 6, no. 4, pp. 1819–1826, Jul. 2015.

[21] T. Zhang, X. Chen, Z. Yu, X. Zhu, and D. Shi, "A Monte-Carlo simulation approach to evaluate service capacities of EV charging and battery swapping stations," *IEEE Trans. Ind. Informat.*, vol. 14, no. 9, pp. 3914–3923, Sep. 2018.

[22] T. Zhang, W. Chen, Z. Han, and Z. Cao, "Charging scheduling of electric vehicles with local renewable energy under uncertain electric vehicle arrival and grid power price," *IEEE Trans. Veh. Technol.*, vol. 63, no. 6, pp. 2600–2612, Jul. 2014.

[23] R. Yu, W. Zhong, S. Xie, C. Yuen, S. Gjessing, and Y. Zhang, "Balancing power demand through EV mobility in vehicle-to-grid mobile energy networks," *IEEE Trans. Ind. Informat.*, vol. 12, no. 1, pp. 79–90, Feb. 2016.

[24] M. Alizadeh, H.-T. Wai, M. Chowdhury, A. Goldsmith, A. Scaglione, and T. Javidi, "Optimal pricing to manage electric vehicles in coupled power and transportation networks," *IEEE Trans. Cont. Netw. Syst.*, vol. 4, no. 4, pp. 863–875, Dec. 2017.

[25] S. Etesami, W. Saad, N. Mandayam, and H. V. Poor, "Smart routing of electric vehicles for load balancing in smart grids," *Automatica*, vol. 120, p. 109148, Oct. 2020.

[26] J. Liu, X. Li, X. Chen, Y. Zhen, and L. Zeng, "Applications of internet of things on smart grid in china," in *13th Int. Conf. Adv. Commun. Tech. (ICACT2011)*, Feb. 2011, pp. 13–17.

[27] H. Tu, Y. Xia, H. H. Iu, and X. Chen, "Optimal robustness in power grids from a network science perspective," *IEEE Trans. Circuits Syst. II*, vol. 66, no. 1, pp. 126–130, Jan. 2019.

[28] C. Sun, X. Wen, Z. Lu, J. Zhang, and X. Chen, "A graphical game approach to electrical vehicle charging scheduling: Correlated equilibrium and latency minimization," *IEEE Trans. Intell. Transp. Syst.*, vol. 22, no. 1, pp. 505–517, Jan. 2021.

[29] D. Li, Q. Yang, D. An, W. Yu, X. Yang, and X. Fu, "On location privacy-preserving online double auction for electric vehicles in microgrids," *IEEE Internet Things J.*, vol. 6, no. 4, pp. 5902–5915, Aug. 2019.

[30] X. Chen, T. Zhang, W. Ye, Z. Wang, and H. H. Iu, "Blockchain-based electric vehicle incentive system for renewable energy consumption," *IEEE Trans. Circuits Syst. II*, vol. 68, no. 1, pp. 396–400, Jan. 2021.

[31] Y. Yu, C. Su, X. Tang, B. Kim, T. Song, and Z. Han, "Hierarchical game for networked electric vehicle public charging under time-based billing model," *IEEE Trans. Intell. Transp. Syst.*, vol. 22, no. 1, pp. 518–530, Jan. 2021.

[32] Y. Zhou, Z. Li, and C. Liu, "The multiobjective based large-scale electric vehicle charging behaviours analysis," *Complexity*, 2018.

[33] Z. Fotouhi, M. Hashemi, H. Narimani, and I. Bayram, "A general model for EV drivers' charging behavior," *IEEE Trans. Veh. Technol.*, vol. 68, no. 8, pp. 7368–7382, Jun. 2019.

[34] California ISO, *California ISO Open Access Same-time Information System*, 2020 (accessed Feb. 10, 2021), https://www.caiso.com/.